Prototyping Directional UAV-based Wireless Access and Backhaul Systems

Mikhail Gerasimenko*, Jiri Pokorny*†, Tibor Schneider*, Jakub Sirjov*, Sergey Andreev†, Jiri Hosek*
*Department of Telecommunications, Brno University of Technology, Brno, Czech Republic
†Unit of Electrical Engineering, Tampere University, Tampere, Finland
Email: mikhail.gerasimenko@tuni.fi, jiri.pokorny@vutbr.cz, xschne06@stud.feec.vutbr.cz, xsirjo00@stud.feec.vutbr.cz, sergey.andreev@tuni.fi, hosek@feec.vutbr.cz

***Abstract*—Providing sufficient mobile coverage during mass public events or critical situations is a highly challenging task for the network operators. To fulfill the extreme capacity and coverage demands within a limited area, several augmenting solutions might be used. Among them, novel technologies like a fleet of compact base stations mounted on Unmanned Aerial Vehicles (UAVs) are gaining momentum because of their time- and cost-efficient deployment. Despite the fact that the concept of aerial wireless access networks has been investigated recently in many research studies, there are still numerous practical aspects that require further understanding and extensive evaluation. Taking this as a motivation, in this paper, we develop the concept of continuous wireless coverage provisioning by the means of UAVs and assess its usability in mass scenarios with thousands of users. With our system-level simulations as well as a measurement campaign, we take into account a set of important parameters including weather conditions, UAV speed, weight, power consumption, and millimeter-wave (mmWave) antenna configuration. As a result, we provide more realistic data about the performance of the access and backhaul links together with the practical lessons learned about the design and real-world applicability of the UAV-enabled wireless access networks.**

I. Introduction

With the ever increasing popularity of social networks and multimedia applications, user data throughput grows significantly in wireless systems. In addition, the community is witnessing the trend of mobile traffic shifting from regular devices to smart devices [1]: by 2022 the ratio of smart and regular devices is expected to be 73 % to 27 %. Smart devices have higher computing resources and network connectivity capabilities, which creates a growing demand for more intelligent networks. Another emerging application is video streaming with the prediction that by 2024 it will comprise 74 % of all mobile data traffic [2]. All these transformations of user behaviour and data traffic demands force mobile operators to augment their infrastructures accordingly.

Providing sufficient network capacity becomes even more challenging during spontaneous events with non-uniform traffic distributions, such as concerts, festivals, and massive outdoor activities, where the number of users clustered in a small area may reach tens of thousands [3]. In such situations, the regular network infrastructure is not capable of handling extreme capacity and coverage demands, so some temporary solutions must be used. Common practice today is the so-called Cell on Wheels (COW) – a mobile base station mounted on a car or a small truck. However, usage of novel technologies like a fleet of compact, fast, and cheap base stations or access points (APs) mounted on Unmanned Aerial Vehicles (UAVs) becomes attractive to offer a possibility of cost-efficient deployment. Example of the corresponding network architecture is shown in Fig. 1, and based on the concept of Integrated Access and Backhaul (IAB) introduced in 3GPP TR 38.874. The document discusses IAB-based network architectures and defines IAB node as "Radio Access Network (RAN) node which supports wireless access to User Equipment (UE) and wirelessly backhauls the access traffic". While the document focuses on scenarios with static IAB nodes, in this paper we propose to enhance IAB architecture by enabling mobility of IAB nodes using UAVs as communication equipment carriers.

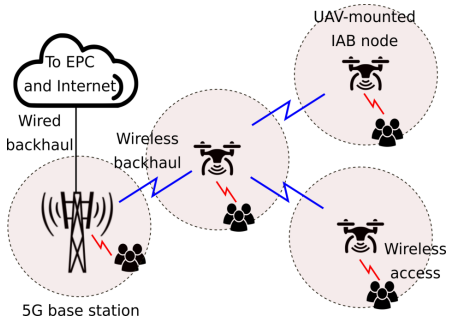

Fig. 1: Concept of UAV-enabled IAB network.

A. Motivation and state-of-the-art background

UAV-assisted networks have been emerging during the last several years because of their mobility and reasonable deployment cost. The concept of aerial wireless access networks was addressed by several research groups. In [4], the authors propose to use aerial base stations, when user data demand exceeds ground RAN capabilities. UAV-assisted networks are also considered in [5], where the authors discuss dynamic behaviour of traffic load and evaluate benefits of moving UAV-mounted base stations. Another work [6] focuses on QoS maximization by finding optimal distance between UAV and users. Optimized deployments of multiple UAVs were also studied in [7] and [8].

As for the implementations, several companies and research groups presented their prototypes of aerial base stations. For example, Google demonstrated a high altitude platform for

extending data coverage in remote areas called Loon [9]. Nokia presented a device called F-Cell – self-configured solar powered aerial small cell capable of providing wireless backhaul with massive MIMO capabilities [10].

B. Problem formulation and contributions

Despite the already available prototypes, there are still many aspects that require further research and testing as was thoroughly described in [11]. Since most of the small size UAVs are designed to use Li-Po or Li-Ion batteries, the matters of energy efficiency and battery life-time are crucial to allow acceptable IAB service time and long-range mobility of the aerial wireless network. As the calculations and measurements show, flight time and possible service time (assuming UAV is hovering while providing network access) depend on several parameters including weather conditions, UAV speed, weight, and power consumption [12], [13]. Also, due to the limitations of UAVs, the installed communication equipment does not provide high network capacity as compared to COW-based systems, which can lead to rapid growth of required aerial base stations in connection with the increasing traffic demands. Moreover, the capacity and range of the aerial network depend on the capabilities of the corresponding communication equipment, which makes attractive the usage of highly-directional interfaces utilizing wider frequency bands.

In this paper, we develop the concept of continuous wireless coverage by the means of UAVs and assess its validity in massive setups with thousands of users. The main contributions of this work are as follows:

- Experimental evaluation of the performance of an aerial wireless network. During this research work, we assembled a prototype of UAV-enabled IAB system, which consists of the following components: Ground Station (GS), UAV-mounted IAB node, and UE.
- Theoretical and experimental evaluation of UAV's hover time. Theoretical part includes a mathematical model to show the impact of ambient temperature, UAV flight speed, and UAV configuration on the available hover time and its comparison with the measurements.
- Analysis that estimates the number of drones required for providing coverage during large public events. It provides the overall assessment of using UAVs as an alternative solution to COWs.

II. Equipment and scenario description

In order to conduct experimental evaluation of the proposed UAV-enabled IAB network, we designed and manufactured the UAV platform, which allows to install custom HW and SW components to complete the defined communication tasks. In this section, all stages of the prototype design are discussed together with practical justifications on selected elements.

A. Baseline equipment

UAVs require several components to be operational: flight controller, motors, propellers, electronic speed controllers (ESC), power supply, and frame. Motor efficiency depends on the UAV structure and mass. The propellers must be selected to provide enough thrust with respect to efficiency. There are various possibilities regarding power supply. Rechargeable batteries are currently vastly used because of their price and high availability. Li-Ion and Li-Po batteries are used for UAV applications due to high energy density reasons (150–250 Wh/kg for Li-Ion or 130-150 Wh/kg for Li-Po) [14]. Another option for power supply is a fuel cell with energy density of two times higher, but also having higher price [15].

Our UAV prototype was constructed from the components listed in Table I. Employed flight controller Radiolink Pixhawk is a popular open-hardware general-purpose autopilot. The Pixhawk was running ArduPilot open-software stack which provides full-featured UAV controller. Frame was a 3D printed copy of DJI F450 from PLA material. Frame draft was modified (upper part was extended) in order to fit the communication equipment. Propellers of size 8045 were used with the above-mentioned frame.

In Table I, power consumption of the components is given. For the motors, this value corresponds to the specification for the particular UAV weight. In our case, the total weight of the UAV is 1.5 kg (0.5 kg of it is a payload). The price of equipment is 870 USD (620 USD excluding payload).

In our deployment, UAV is flying in unmanned mode driven by FlytOS installed on the on-board Raspberry Pi (RPi). FlytOS is a proprietary software framework, which works along with Robot Operating System (ROS) running on Linux, and suits for scalable drone applications. FlytOS offers APIs and SDKs to create applications like delivery, aerial photography, or research.

B. IAB enablers

3GPP's TR 38.874 defines architectural strategies, use cases, and deployment scenarios for the IAB-enabled networks. According to this report, the options for the IAB node transceivers include out-of-band and in-band backhauling, which means that backhaul can utilize different/same frequency band with appropriate MAC-layer modifications. Moreover, the document discusses options for access and backhaul radio technologies, mostly concentrating on different combinations of 5G New Radio (NR) and LTE. However, the definition of IAB node introduced in the document does not limit the system designer to 3GPP-only technologies. For that reason, and due to the absence of the appropriate NR equipment on the market, we decided to use Mikrotik wAP 60G (802.11ad) as a backhaul link and RPi model 3B+ equipped with 5 GHz 802.11ac WiFi as a user access provider.

TABLE I: UAV prototype components list

Component	Model	Power cons. (max)
Flight controller	Pixhawk 2.4.8	2 W
Motors	EMAX MT2213 KV935	60 W
Battery	14.8V 4000 mAh 25C	-
GPS module	NEO-M8N	$<$1 W
RC(RX)	FS-iA10B	$<$1 W
Backhaul comm.	Mikrotik wAP 60G	5 W
Access comm.	Raspberry Pi 3B+	1.5 W

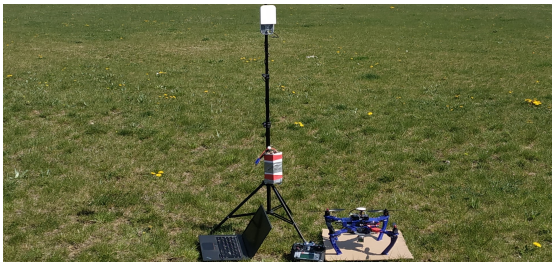

(a) Equipment used for measurements

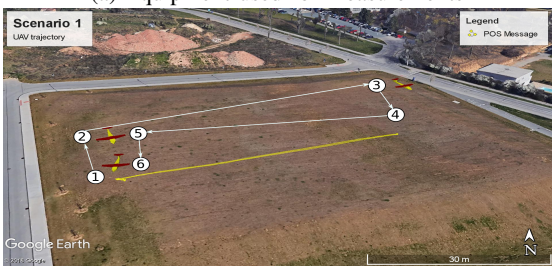

(b) Scenario one mobility plan

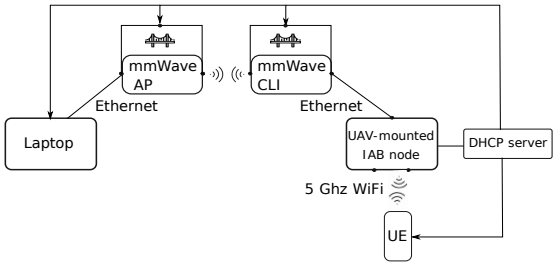

(c) Prototype network plan

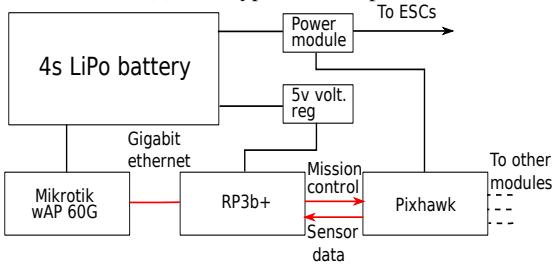

(d) UAV communication equipment composition

Fig. 2: Prototype network details

The overall prototype network structure and interconnection of the modules on the UAV side are shown in Fig. 2a to 2d respectively. RPi is powered through a separate voltage regulator, while Mikrotik device has its own internal voltage regulator. The mmWave antenna array is installed on the right side of the UAV.

C. Scenarios of interest

In this paper, we concentrate on two core scenarios targeting performance of the prototype network and capabilities of the UAV in terms of power consumption and flight time. For simplicity, we call these two setups "scenario one" and "scenario two".

The layout of scenario one is shown in Fig. 2b. Initially, the UAV with installed telecommunication equipment is located at point 1, while GS station is located five meters away from the UAV. UE is located at the ground level at point 3 during all measurements.

At the beginning, the UE is trying to connect to the UAV AP. After initiation of statistics collection on the GS, the operator is triggering the start of the way-point following mission on the RPi. The flight plan itself includes several steps: takeoff to five meters of altitude; align UAV yaw; fly to the position defined by the GPS coordinates (60 m from GS); hover for two minutes; return to the start position; land. During the flight, UAV's maximum horizontal speed is fixed to 4 m/s and flight altitude is 5 m. In-flight yaw alignment (Fig. 2b) is performed to direct the UAV mmWave antenna array towards the GS (drone starboard is always aimed towards GS).

In the second scenario, we measure and calculate the UAV flight time when all communication equipment is enabled, assuming specific flight plan created to match the realistic IAB scenarios. First, the UAV performs takeoff to the altitude of 5 m, then flies for the fixed distance and starts hovering, providing service to the UE. During several experiments, we changed various parameters of the scenario and measured how long can UAV provide access service until battery discharges to a certain level.

Finally, based on the results from scenarios one and two, we created a simple system-level model, in order to scale the obtained results to multi-UE deployments.

III. Conceptual Analysis

A. Energy efficiency

Flight time of a UAV is influenced by many factors from which the most important ones are power consumption and payload weight. To calculate the UAV-enabled AP service time, the following parameters must be taken into account: battery capacity C_b, drone mass m, and ambient temperature τ. To determine the energy availability for hover time, the flight has to be divided into specific phases: (i) ascend, (ii) descend, (iii) horizontal flight, and (iv) hover. Energy consumption calculations were derived from the current consumption of each motor provided by its manufacturer based on the actual motor thrust $I(T)$. In this section, the following quantities will be used: m – UAV mass, a – UAV acceleration, F_g – gravitational force, g – gravitational acceleration, d – distance, and v – UAV speed.

Drag force for ascending is calculated as $F_a = ma + F_g + F_{air}$, where F_{air} is air resistance force. This equation can be developed into $F_a = ma + mg + \frac{\rho}{2} c_d S v^2$, where ρ is air density, c_d is drag coefficient, and S is a front surface of the UAV. Drone acceleration is obtained from equation $a = (N_m T_{max} g - mg - \frac{\rho}{2} c_d S v^2)/m$. This equation calculates the maximum acceleration the UAV can achieve. N_m is number of motors and T_{max} is maximum thrust of a single motor. During horizontal flight, three forces are impacting the UAV, F_g, F_a, and F_s. For the UAV to move sideways, F_g and F_a must be equal. Resulting thrust force is calculated as $F_s = ma + \frac{\rho}{2} c_d S v^2$. Hovering is similar to horizontal flight, with forces

$F_g = F_a$, and $F_h = F_g$. Descending process is similar to ascending, except that force $F_a < F_g$. Finally, after obtaining thrust forces for all flight phases, thrust itself can be calculated as $T = \frac{F}{g}$ and current for each phase can be obtained from the available $I(T)$ characteristics.

Total UAV flight time consists of partial times throughout the entire mission $t = t_a + t_s + t_d + t_h$, where t_a is ascending time, t_s is horizontal flight time, t_d is descending time, and t_h is hover time. Time of each phase (except hover time) is calculated as $t = \frac{d}{v}$. Total charge required for each mission is designated as Q and is calculated as $Q = Q_a + Q_s + Q_h + Q_d + Q_r$, from which the resulting hover time is equal to $Q_h = Q - Q_a - Q_s - Q_d - Q_r$. Here, Q_r is reserved energy – if Li-Po batteries are used, it is also necessary that battery charge state does not drop below 30 % of full capacity [14]. Ambient temperature also affects battery capacity – battery capacity model from [13] was used to take it into account: $C_b = 0.8814 + 0.0091\tau - 0.0001\tau^2$. When calculating the available charge for hovering Q_h, the total charge Q is substituted with C_b. Total hover time available for a specific mission is then equal to $t_h = \frac{Q_h}{I_h}$.

B. System-level analysis

Second part of the analysis describes the scenario where multiple users N_u participate in a crowded outdoor event. In this setup, we assume that drones are already deployed in the required area and can provide service from the moment of their takeoff. The maximum distance, to which drones can be deployed is then limited by the drone configuration. Here, we also assume that there are re-charging pads installed in the deployment area, allowing to recharge the desired number of UAVs without the need to return to the initial takeoff location. Finally, here we concentrate on the performance of the access link, assuming that the backhaul link can always provide higher throughput, regardless of the distance between deployment area and GS.

Each user requires throughput C_u. The capacity provided by the access link on one UAV is designated as C_s. Maximum number of users per BS is defined as $N_b = \frac{C_s}{C_u}$. MAC layer features and interference are not taken into account – although it is an important limitation of our model, in this paper we concentrate on more general aspects of the system planning, and thus leave these issues for future research.

Number of drones deployed for continuous coverage is calculated as $N_d = N_u \frac{C_u}{C_s}$. However Li-Po powered drones have very limited flight time and cannot provide continuous coverage throughout the entire event that can last for several hours or days. Therefore, it is necessary to determine the minimum number of drones per location N_l taking into account the hover and recharge times. Assuming uninterrupted service, this value can be calculated as $N_l = \left\lceil \frac{t_r}{t_h} \right\rceil + 1$, where t_r is the time required to recharge the battery and t_h is the time UAV is capable of hovering in one position. Finally, the total minimum number of UAVs required over the entire area is calculated as $N_t = N_l N_d$.

IV. Evaluation of results

A. Scenario one

In scenario one, performance of both access and backhaul links was evaluated. The backhaul link antenna array installed on the UAV is fixed perpendicular to the plane of horizon.

Measurements were conducted under automated flight with the operator standing by for cases of emergency takeover. During measurements, the following statistics were collected: RSSI for both access and backhaul links (Fig. 3a), backhaul PHY rate, end-to-end (UE-GS) throughput measured with iPerf (Fig. 3b), and GS antenna array configuration setup in terms of elevation and azimuth angles (Fig. 3c). Trajectory points from Fig. 2b are mapped onto the measurements timeline (x axis in all plots) as it is shown in Fig. 3a.

In Fig. 3a, RSSI values for access and backhaul links are shown together with TX PER, measured at the GS w60g device. As expected, before mission starts, RSSI for backhaul link is high, despite the antennas not being oriented towards each other. The mismatch is compensated by changing the array configuration (elevation and azimuth of the main lobe, Fig. 3c). In the plot, zero value for elevation means that the main lobe is parallel to horizon, while positive/negative numbers for the elevation and azimuth mean up/down and left/right tilt of the current configuration. Surprisingly, GS antenna is not utilizing the line-of-sight (LOS) ray – in that case the elevation should be negative, due to the fact that UAV is located on the ground level, while GS antenna is fixed at 1.5 m height. At the takeoff and until the UAV reaches point 3 and starts to hover above the UE area, there are variations in the chosen antenna configuration, followed by the growing TX PER. However, when the UAV switches to hovering state, PER is becoming stable, together with RSSI and PHY rate (around 1 Gbps).

On the access link, the RSSI statistics also follow a predictable pattern – at the start, connection is barely stable, and when the UAV arrives at point 3 both RSSI and end-to-end throughput reach their maximum. Unfortunately, software and hardware limitations do not allow to experience more than 30 Mbps using RPi 3b+ with the particular operating system installed (max PHY rate achieved over the allowed 20 MHz bandwidth is 54 Mbps). On top of that, the absence of external antenna makes the access link particularly vulnerable to user and UAV mobility as well as self-blockage (LOS blockage by the UAV itself), which can be visible as both throughput and RSSI drop even when the UAV is hovering. We recommend to use other hardware if performance of access link is a key metric. Despite those limitations in this scenario, we confirmed that UAV can be used as a mobile carrier of IAB node, assuming the UAV remains static when providing access service.

B. Scenario two

In this scenario, the capabilities of UAV-based IAB node in terms of service time are evaluated and discussed. Moreover, at the end of this subsection we offer an example on how this time differs for variable UAV configurations.

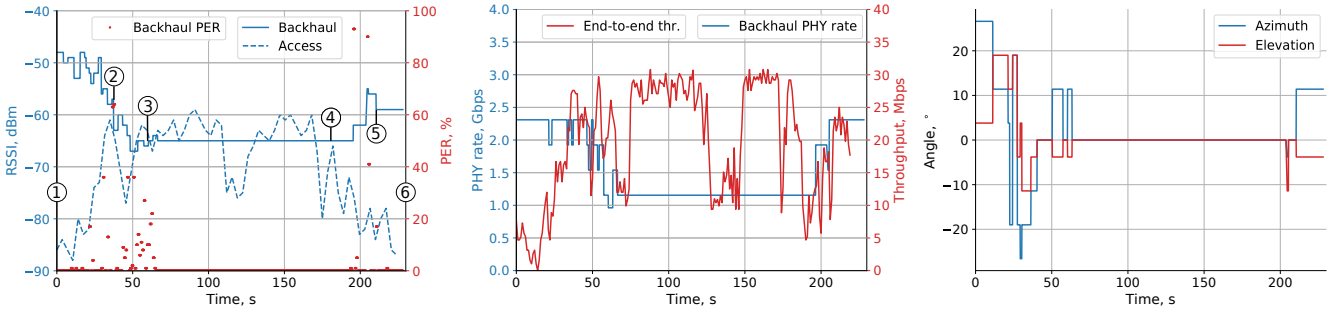

(a) Backhaul and access link RSSI, TX packet error rate

(b) Backhaul PHY rate, end-to-end throughput

(c) Ground station antenna array configuration.

Fig. 3: Scenario one: communication equipment performance evaluation.

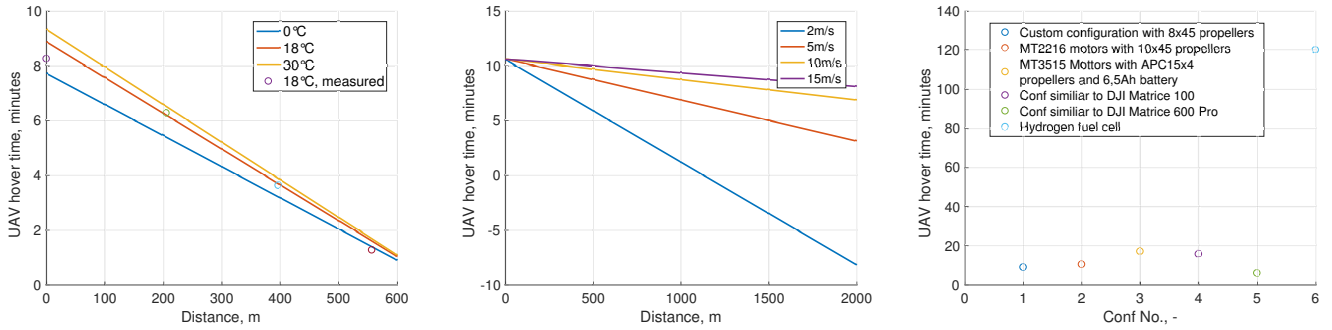

(a) Hover time in different temperature conditions

(b) Hover time for different UAV speeds

(c) Hover time for different UAV configurations.

Fig. 4: Scenario two: power consumption evaluation.

In Fig. 4a, a comparison of the expected hover time and measurements is provided. It should be noted that the measurements were conducted in certain weather conditions (18 °C, around 4 m/s wind speed, no rain). UAV speed for this plot was fixed to 1.6 m/s. For safety reasons, in this setup the drone was flying to the destination point located at a particular distance from the origin, and untill battery level reached 50 %. This value was selected instead of 30 % for security purposes, because in the past we experienced energy fluctuations and the experimental UAV had problems with stable flight. After that, UAV was programmed to perform landing without returning to the initial position. Closer comparison of the results shows a reasonable match between theory and practice, despite some minor variations for the first and the last measurement points caused by fluctuations of the trajectory and weather conditions, together with the non-ideal behaviour of the Li-Po battery.

When the theoretical model was verified, we conducted the calculations for different temperatures, in order to observe how weather conditions can affect the performance of the network. Results in Fig. 4a suggest that the temperature has a significant impact on the scenarios in which UAV is hovering more than moving.

In Fig. 4b, a similar comparison is made for different UAV speeds (temperature is fixed to 25 °C). In this setup, we allow UAV to discharge its battery to 30 % level. Here, significant performance difference can be observed, and we can conclude that it is often preferred to travel at the maximum achievable speed, in order to maximize the available service time.

Finally, we compare the hover time for different UAV types, assuming the UAV speed of 15 m/s, 25 °C temperature, travel distance of 1 km, and landing trigger set to 30 % battery level. Fig. 4c shows differences between the hover times for different UAV configurations. On top of the three custom UAV configurations (No. 1, 2, and 3), we considered two commercially available UAVs, a quadcopter DJI Matrice 100 (No. 4), and a hexacopter DJI Matrice 600 Pro (No. 5). These configurations differ from one another only by body shape, motor type, and propellers. Each motor type achieves different energy efficiency with different propeller types and that reflects on the resulting hover time. According to our calculations, by using Li-Po batteries we can obtain the hover time of up to 18 minutes. Lastly, we included an example implementation of a hydrogen fuel cell (No. 6) used in [16] with 2 h of declared flight time. However, it should be taken into account that the UAVs differ also in the maximum achievable speeds, prices, and payload weight. E.g., the mentioned hexacopter can carry up to 10 kg, allowing to install more advanced long-range transceivers.

C. System-level results

In this subsection, we assess the number of UAVs required to satisfy the capacity demands in a system-level scenario.

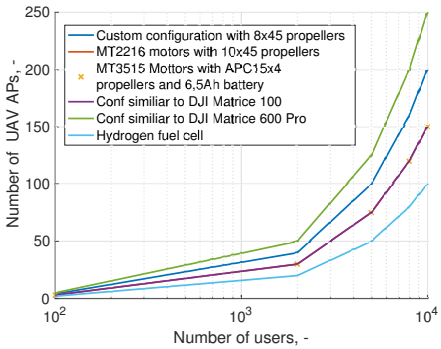

Fig. 5: Number of UAVs required for different number of UEs.

Coverage requirements of the deployment are not considered for this case, and the total number of drones N_t depends only on the number of users N_u and the recharge time t_r. Table II introduces the list of parameters used for this calculation. The recharging station was located within 100 m, while the energy consumption required for reaching the area was disregarded. Calculations were made for N_u between 100 and 10 k. Each user requires the throughput of 5 Mbps, which is a typical value for video streaming[1]. Considered wireless technology for both access and backhaul is 60 GHz mmWave. The limiting throughput value for both networks is set to 1 Gbps. This value was selected from the commercially available devices that had dimensions and mass low enough for a small-size UAV to carry. The output is shown in Fig. 5. Resulting N_t differences are caused by varying maximum flight time for each configuration. Hover time values in every case were taken from the scenario two (see Fig. 4c).

TABLE II: System-level parameters used for calculation

Parameter	Value	Definition
C_u	5 Mbps	Required throughput per UE
N_u	100 – 10 k	Number of users in scenario
C_s	1 Gbps	Available throughput per BS
t_r	60 min	Recharge time

V. Conclusion

In this research work, we have addressed the highly emerging topic of UAV-enabled wireless access networks. To provide realistic measurement data, we have designed and prototyped our own UAV platform augmented with the telecommunication equipment that enables mobile service via mmWave. With extensive experimental as well as simulation-based evaluations, we have confirmed the overall usability of this technology and offered several valuable insights into its practical deployment. Among them, we would like to highlight that the energy efficiency of the entire scenario is a critical issue especially for Li-Po battery powered UAVs. In connection to that, the maximum flying distance from the original takeoff position to the operating area is limited, and therefore reliable charging strategies should be proposed. Another possible limitation is the length and reliability of the backhaul link. Here, it is necessary to emphasize that high-directivity antenna array systems, which in theory could enable long-range communications with low interference and TX power, in practice lack low-complexity beam-search algorithms, able to work with fast-moving objects. To increase backhaul link length, network can also be extended for a multi-UAV scenario with some UAVs serving as a relay between the GS and others. This scenario will be targeted in our future research and includes the tasks of drone positioning, architecture choice (e.g., ad-hoc vs. infrastructure), and routing.

[1]Ericsson mobility report, June, 2017.

Acknowledgment

The described research was supported by the National Sustainability Program under grant LO1401 as well as by the project 5G-FORCE and the aColor project (Autonomous and Collaborative Offshore Robotics). For the research, the infrastructure of the SIX Center was used. This paper is also based upon support of international mobility project MeMoV, No. CZ.02.2.69/0.0/0.0/16_027/00083710 funded by European Union, Ministry of Education, Youth and Sports, Czech Republic and Brno, University of Technology.

References

[1] Cisco, "Cisco Visual Networking Index: Global Mobile Data Traffic Forecast Update, 2017-2022 White Paper," February 18, 2019.
[2] Ericsson, "Ericsson mobility report," June, 2019.
[3] N. D. Mickulicz, U. Drolia, P. Narasimhan, and R. Gandhi, "Zephyr: First-person wireless analytics from high-density in-stadium deployments," in *17th International Symposium on A World of Wireless, Mobile and Multimedia Networks (WoWMoM)*, pp. 1–10, IEEE, 2016.
[4] V. Sharma, M. Bennis, and R. Kumar, "UAV-assisted heterogeneous networks for capacity enhancement," *IEEE Communications Letters*, vol. 20, no. 6, pp. 1207–1210, 2016.
[5] S. Mignardi and R. Verdone, "On the performance improvement of a cellular network supported by an unmanned aerial base station," in *29th International Teletraffic Congress*, vol. 2, pp. 7–12, IEEE, 2017.
[6] A. V. Savkin and H. Huang, "Deployment of unmanned aerial vehicle base stations for optimal quality of coverage," *IEEE Wireless Communications Letters*, vol. 8, no. 1, pp. 321–324, 2019.
[7] B. Galkin, J. Kibilda, and L. A. DaSilva, "Deployment of UAV-mounted access points according to spatial user locations in two-tier cellular networks," in *2016 Wireless Days (WD)*, pp. 1–6, IEEE, 2016.
[8] J. Lyu, Y. Zeng, R. Zhang, and T. J. Lim, "Placement optimization of UAV-mounted mobile base stations," *IEEE Communications Letters*, vol. 21, no. 3, pp. 604–607, 2017.
[9] Google X, "Balloon-powered Internet for everyone," 2019.
[10] Nokia, "F-Cell technology from Nokia Bell Labs revolutionizes small cell deployment by cutting wires, costs and time," October 3, 2016.
[11] A. Fotouhi, H. Qiang, M. Ding, M. Hassan, L. G. Giordano, A. Garcia-Rodriguez, and J. Yuan, "Survey on UAV cellular communications: Practical aspects, standardization advancements, regulation, and security challenges," *IEEE Communications Surveys & Tutorials*, 2019.
[12] Y. Chen, D. Baek, A. Bocca, A. Macii, E. Macii, and M. Poncino, "A Case for a Battery-Aware Model of Drone Energy Consumption," in *International Telecommunications Energy Conference*, pp. 1–8, IEEE, 2018.
[13] S. J. Kim, G. J. Lim, and J. Cho, "Drone flight scheduling under uncertainty on battery duration and air temperature," *Computers & Industrial Engineering*, vol. 117, pp. 291–302, 2018.
[14] N. K. Ure, G. Chowdhary, T. Toksoz, J. P. How, M. A. Vavrina, and J. Vian, "An automated battery management system to enable persistent missions with multiple aerial vehicles," *IEEE/ASME Transactions on Mechatronics*, vol. 20, no. 1, pp. 275–286, 2015.
[15] K. Celik and H. Eren, "UAV fuel preferences for future cities," in *6th International Istanbul Smart Grids and Cities Congress and Fair (ICSG)*, pp. 151–154, IEEE, 2018.
[16] EnergyOR Technologies, "H2QUAD 400," 2019.